SCIENCE CHINA
Information Sciences

• MOOP •

March 2022, Vol. 65 134201:1–134201:3
https://doi.org/10.1007/s11432-020-3054-7

Modeling and analysis of an underwater biomimetic vehicle-manipulator system

Xuejian BAI[1,2], Yu WANG[2*], Shuo WANG[1,2,3], Rui WANG[2], Min TAN[1,2] & Wei WANG[4]

[1]*School of Artificial Intelligence, University of Chinese Academy of Sciences, Beijing* 100049*, China;*
[2]*State Key Laboratory of Management and Control for Complex Systems, Institute of Automation, Chinese Academy of Sciences, Beijing* 100190*, China;*
[3]*CAS Center for Excellence in Brain Science and Intelligence Technology, Shanghai* 200031*, China;*
[4]*School of Control Science and Engineering, Shandong University, Jinan* 250061*, China*

Received 15 May 2020/Revised 24 July 2020/Accepted 1 August 2020/Published online 1 September 2021

Citation Bai X J, Wang Y, Wang S, et al. Modeling and analysis of an underwater biomimetic vehicle-manipulator system. Sci China Inf Sci, 2022, 65(3): 134201, https://doi.org/10.1007/s11432-020-3054-7

In recent years, underwater vehicle-manipulator systems (UVMSs) have captured researchers' attention. Inspired by fish, bionic mechanisms were introduced into a UVMS. The underwater biomimetic vehicle-manipulator system (UBVMS) is actuated by two symmetrically arranged biomimetic undulatory fin propulsors [1]. Based on the UBVMS, some topics have been researched, such as free-floating autonomous operation [2,3], three-dimensional helical path following [4], and underwater video processing [5]. An accurate mathematical model is beneficial to the coordinated control of the UBVMS. Therefore, this article dedicates on the study of hydrodynamic model and analysis for the UBVMS, involving an identification of hydrodynamic coefficients of the UBVMS, the hydrodynamic analysis of the manipulator, and the hydrodynamic analysis of the undulatory fin propulsors.

Identification of hydrodynamic coefficients. In this study, computational fluid dynamics (CFD) technology is applied to determine the hydrodynamic coefficients. The hydrodynamic coefficients are nondimensionalized with characteristic length L and water density ρ. The dimensionless hydrodynamic model expression of the UBVMS can be described with 84 hydrodynamic coefficients. A spatial captive motion approach [6] is proposed to simulate the 6-degree of freedom (DOF) motion of the UBVMS efficiently. By defining 6 different irregular disturbances in 6 DOFs of the UBVMS, the velocity and accelerated velocity of each DOF are nonzero and irregular. The spatial captive motion can be described as follows:

$$V = V_0 + V_{\mathrm{p}} \sin(2\pi f_{V1} t) \sin(2\pi f_{V2} t), \tag{1}$$

where V denotes any one of velocities in the 6 DOFs. V_0 denotes a constant velocity. V_{p} denotes the disturbance amplitude. f_{V1} and f_{V2} represent the disturbance frequencies.

Simulations are implemented in Fluent software. According to the hydrodynamic forces and moments X, Y, Z, K, M and N obtained from Fluent, multiple linear regression is used to identify the hydrodynamic coefficients and derive the hydrodynamic model. Comparison between Fluent data and model data indicates that the model matches well with the Fluent result. However, some discrepancies appear in the crests and troughs, which mainly result from two potential reasons. First, the couple effects of 6-DOF motions are contributed to the hydrodynamic forces and moments, but they are neglected in the hydrodynamic model. Second, during the CFD calculation, the dynamic mesh technology changes the mesh at each step, which causes some low-quality mesh and results in unpredictable simulation errors.

Hydrodynamic analysis of the manipulator. The hydrodynamic of the manipulator has adversely effect on the accuracy and speed of underwater operations. The manipulator of the UBVMS has 5 joints, namely Waist joint, Shoulder joint, Elbow joint, Wrist pitch joint and Wrist roll joint. As shown in Figure 1(a), θ_1, θ_2, θ_3, θ_4, and θ_5 denote the angle of each joint. It is worth noting that the definitions of the joints' rotation directions obey the right hand rule in the corresponding coordinate systems in Figure 1(a).

Waist joint rotates around the Z-axis. Figure 1(b) shows the simulated hydrodynamic forces with the Waist joint rotating at different rotation velocities. In Figure 1(b1) and (b2), the rotation directions of Waist joint are positive from 0° to 360°, and in Figure 1(b3) and (b4), the rotation directions of Waist joint are negative from 360° to 0°. It is observed that the hydrodynamic forces increase with the enhancement of the joint's rotation velocity, which exceed 10 N at 50°/s and are almost zero at 5°/s. In addition, it is shown that the x-direction hydrodynamic forces have the same variation trend at positive and negative rotation directions, while y-direction hydrodynamic forces show inverse variation trend at positive and negative rotation directions.

Figure 1(c) shows the simulated results at rotation veloc-

* Corresponding author (email: yu.wang@ia.ac.cn)

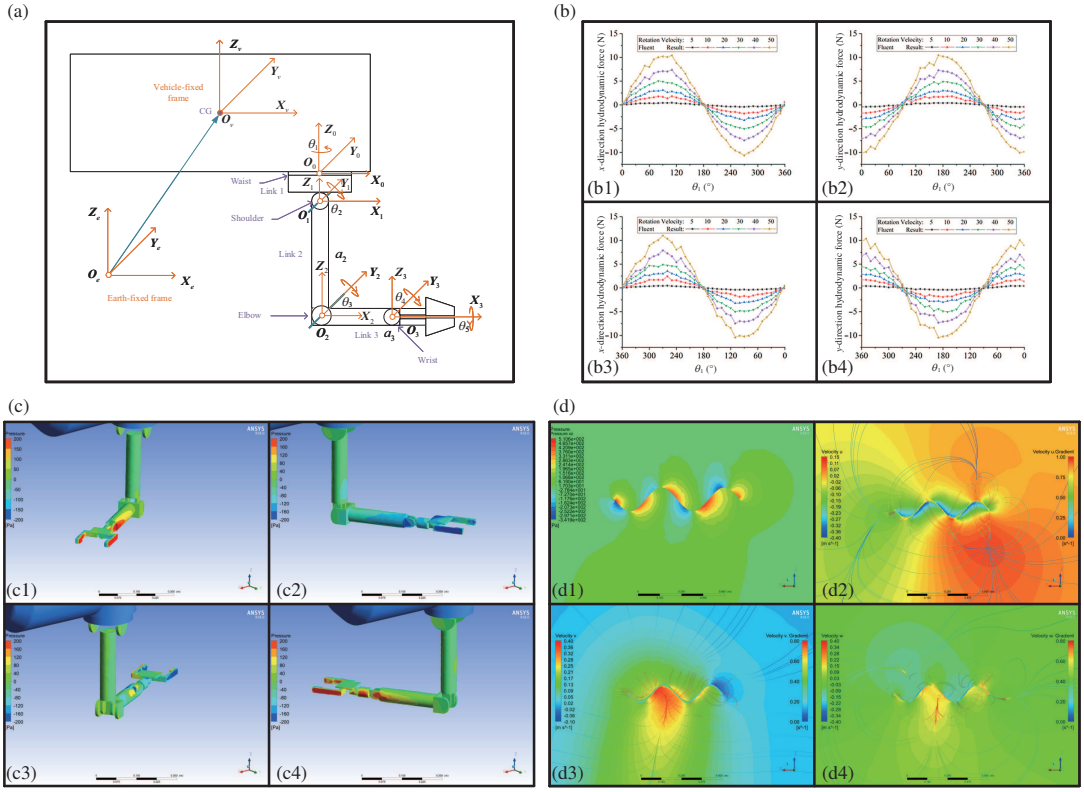

Figure 1 (Color online) (a) Coordinate frames for the UBVMS model; (b) hydrodynamic forces caused by rotation of Waist joint; (c) pressure distribution of manipulator with Waist joint rotation at: (c1) 30° (c2) 120° (c3) 210° (c4) 300°; (d) simulation results on the $O-xz$ section of flow field ($t/T=0.5$).

ity of Waist joint being 30°/s and rotation direction being positive. It is observed that the facing-flow side of the manipulator sustains positive pressure (red part in Figure 1(c1) and (c4)) and the backing-flow side of manipulator is subjected to negative pressure (blue part in Figure 1(c2) and (c3)). As a result, the pressure difference exerts hydrodynamic forces on the manipulator, which can be decomposed into sinusoidal x-direction and y-direction hydrodynamic forces shown in Figure 1(b). The detailed analysis of other joints are demonstrated in the presentation slides.

Hydrodynamic analysis of the undulatory fin propulsors. The manipulator causes continuous and relatively small disturbance. Hence continuous and small forces are needed to compensate the disturbance. Knifefishes can produce highly stable small forces with undulatory fins. In recent years, the motions of knifefishes have attracted much attention and the undulatory fin propulsor has been presented [7]. However, due to the complicated hydrodynamic effects, further efforts are needed to study the dynamic mechanism of undulatory fin propulsor. We implemented CFD simulation to analyze the hydrodynamics of the undulatory fin propulsors.

The UBVMS is actuated by two symmetrically arranged undulatory fin propulsors, which compose a bio-inspired mechatronic system. Each undulatory fin propulsor consists of 12 fin rays controlled by servo motors. The undulating motion of each fin ray can be described as

$$\beta_i = \beta_m \sin[2\pi(ft + x_i/\lambda) + \phi_0] + \beta_B,\ i = 1, 2, \ldots, 12, \quad (2)$$

where β_m denotes maximum angular deflection of the sinusoidal waves, f denotes oscillating frequency, t denotes time, λ denotes the wave length, ϕ_0 denotes the initial phase, β_i and x_i represent the deflection angle and the position of the ith fin ray, respectively; and β_B denotes the deflection angle of the undulatory fin propulsor.

The fluid pressure $F_p(t)$ and fluid drag $F_d(t)$ are described as

$$F_p(t) = \sum F_{pi}(t) = \int_S \boldsymbol{p}(t) \cdot \mathrm{d}S, \quad (3)$$

$$F_d(t) = \sum F_{di}(t) = \mu \int_S \left(\frac{\partial \boldsymbol{v}_{\mathrm{fluid}}(t)}{\partial \delta} \right) \Big|_{\delta=0} \mathrm{d}S, \quad (4)$$

where $F_{pi}(t)$ and $F_{di}(t)$ represent the fluid pressure and fluid drag on the ith element, respectively; $\boldsymbol{p}(t)$ denotes the stress vector; S denotes the wetted surface area; μ denotes the kinetic viscosity of fluid; $\boldsymbol{v}_{\mathrm{fluid}}(t)$ denotes the velocity vector of the boundary layer; $\frac{\partial \boldsymbol{v}_{\mathrm{fluid}}(t)}{\partial \delta}$ denotes the normal velocity gradient.

Finally, the thrust force $X_{\mathrm{Fin}}(t)$, the yawing force $Y_{\mathrm{Fin}}(t)$ and the lift force $Z_{\mathrm{Fin}}(t)$ can be derived as follows:

$$\begin{cases} X_{\mathrm{Fin}}(t) = \displaystyle\int_S p(t)(\boldsymbol{n}_x \cdot \mathrm{d}S) \\ \qquad\qquad - \mu \displaystyle\int_S \left(\frac{\partial \boldsymbol{v}_{\mathrm{fluid}}(t)}{\partial \delta} \cdot \boldsymbol{n}_x \right) \Big|_{\delta=0} \mathrm{d}S, \\ Y_{\mathrm{Fin}}(t) = \displaystyle\int_S p(t)(\boldsymbol{n}_y \cdot \mathrm{d}S) \\ \qquad\qquad - \mu \displaystyle\int_S \left(\frac{\partial \boldsymbol{v}_{\mathrm{fluid}}(t)}{\partial \delta} \cdot \boldsymbol{n}_y \right) \Big|_{\delta=0} \mathrm{d}S, \\ Z_{\mathrm{Fin}}(t) = \displaystyle\int_S p(t)(\boldsymbol{n}_z \cdot \mathrm{d}S) \\ \qquad\qquad - \mu \displaystyle\int_S \left(\frac{\partial \boldsymbol{v}_{\mathrm{fluid}}(t)}{\partial \delta} \cdot \boldsymbol{n}_z \right) \Big|_{\delta=0} \mathrm{d}S, \end{cases} \quad (5)$$

where $\boldsymbol{n}_x$, $\boldsymbol{n}_y$, and $\boldsymbol{n}_z$ represent the unit vector in the x, y, and z direction, respectively.

Simulation results on the $O-xz$ section of the flow field are presented in Figure 1(d). In Figure 1(d1), the pressure on the $-x$ side of the crests is positive and on the $+x$ side is negative, because the hydrodynamic forces are along the $+x$ direction. In Figure 1(d2), the x-component velocity of the flow near the fin surface is larger than that away from the fin surface, because the wave transmitting along the $-x$ direction exerts reaction on the fluid. Besides, the vortex caused by fluctuation disturbs the hydrodynamic effects.

In Figure 1(d3) and (d4), the y-component velocity is positive, which indicates that the fluctuation causes yawing force along the $-y$ direction. The z-component velocity presents asymmetrically and the fluctuation generates lift force along the $+z$ direction.

Experimental verification. To verify the computational model, a measurement platform is designed and forward swimming experiments are carried out to measure the forces generated by an undulatory fin propulsor and the motion data during the UBVMS's forward motion. The experimental results show that the model data are consistent with the measured data, which indicates that the proposed dynamic model and the hydrodynamic coefficients identification method are feasible and effective.

Acknowledgements This work was supported by National Natural Science Foundation of China (Grant Nos. U1713222, 61703401, U1806204), in part by Foundation for Innovative Research Groups of National Natural Science Foundation of China (Grant No. 61421004), and in part by Youth Innovation Promotion Association CAS.

Supporting information Videos and other supplemental documents. The supporting information is available online at info.scichina.com and link.springer.com. The supporting materials are published as submitted, without typesetting or editing. The responsibility for scientific accuracy and content remains entirely with the authors.

References

1 Tang C, Wang R, Wang Y, et al. RobCutt: a framework of underwater biomimetic vehicle-manipulator system for autonomous interventions. In: Proceedings of the 14th International Conference on Automation Science and Engineering, Munich, 2018. 477–482
2 Tang C, Wang Y, Wang S, et al. Floating autonomous manipulation of the underwater biomimetic vehicle-manipulator system: methodology and verification. IEEE Trans Ind Electron, 2018, 65: 4861–4870
3 Wang Y, Wang S, Wei Q P, et al. Development of an underwater manipulator and its free-floating autonomous operation. IEEE/ASME Trans Mechatron, 2016, 21: 815–824
4 Wang R, Wang S, Wang Y, et al. Three-dimensional helical path following of an underwater biomimetic vehicle-manipulator system. IEEE J Ocean Eng, 2017, 43: 391–401
5 Tang C, von Lukas U F, Vahl M, et al. Efficient underwater image and video enhancement based on Retinex. Signal Image Video Process, 2019, 13: 1011–1018
6 Ting G, Pang Y, Wang Y, et al. Calculation method of hydrodynamic coefficients for underwater vehicles. J Harbin Eng Univ, 2019, 40: 174–180
7 Wang S, Wang Y, Wei Q P, et al. A bio-inspired robot with undulatory fins and its control methods. IEEE/ASME Trans Mechatron, 2017, 22: 206–216